

**Modeling inhomogeneous van der Waals fluids using an analytical direct correlation function**

Yiping Tang\*

*Honeywell Process Solutions, 300-250 York Street, London, Ontario, Canada N6A 6K2*

Jianzhong Wu

*Department of Chemical and Environmental Engineering, University of California, Riverside, California 92521-0425, USA*

(Received 16 January 2004; published 23 July 2004)

Rosenfeld's perturbative method [J. Chem. Phys. **98**, 8126 (1993)] for constructing the Helmholtz energy functional of classical systems is applied to studying inhomogeneous Lennard-Jones fluids, in which the key input—the bulk direct correlation function—is obtained from the first-order mean-spherical approximation (FMSA) [J. Chem. Phys. **118**, 4140 (2003)]. Preserving its high fidelity at the bulk limit, the FMSA shows stable and satisfactory performance for a variety of inhomogeneous Lennard-Jones fluids including those near hard walls, inside slit pores, and around colloidal particles. In addition, the inhomogeneous FMSA reproduces reliably the radial distribution function at its bulk limit. The FMSA is found, in particular, much better than the mean-field theory for fluids near hard surfaces. Unlike alternative non-mean-field approaches, the FMSA is computationally as efficient as the mean-field theory, free of any numerical determination of structure information, weight functions, or empirical parameters.

DOI: 10.1103/PhysRevE.70.011201

PACS number(s): 61.20.Gy, 05.70.Np, 82.60.Qr, 71.15.Mb

**I. INTRODUCTION**

Inhomogeneous fluids with both repulsive and attractive intermolecular forces have been active research subjects, because they often serve as a benchmark to study a variety of interesting problems such as interfacial phenomena, surface adsorption, wetting, capillary condensation, etc. Today, the most promising method to handle these systems seems to be the classical density-functional theory (DFT), which treats the Helmholtz free energy as a function of density distribution. DFT has enjoyed some remarkable successes [1] for fluids with solely repulsive forces. One example is provided by the fundamental measure theory (FMT) for inhomogeneous hard spheres proposed by Rosenfeld over a decade ago [2–4]. In particular, the latest modified fundamental measure theory (MFMT) yields very accurate density profiles for hard spheres near walls and inside slit pores as well as the correlation functions for homogeneous hard spheres and mixtures [5–8]. In contrast, DFT theories for fluids with an attractive component in the intermolecular potential, as typically represented by the Lennard-Jones (LJ) potential, are less satisfactory. Even to date, the most popular method for the dispersion force remains to be the van der Waals (VDW) or mean-field theory (MFT). MFT is computationally efficient and can describe qualitatively some inhomogeneous phenomena. Nevertheless, the inherited problems are standing: it neglects the fluid structure completely and its performance is highly system-dependent. For instance, in comparison with simulation results, the density profiles predicted by MFT appear satisfactory for LJ fluids confined in attractive slit pores, but the prediction is very poor when they are near a hard surface. The deficiencies of MFT can be immediately recog-

nized by the fact that at the homogeneous limit the DFT is reduced to the well-known VDW equation of state, which is only qualitative for the phase diagram and chemical potential calculations. Both properties are vital to any study of inhomogeneous fluids [9].

Earlier efforts to remedy the MFT resorted to some modifications [10,11] of the effective hard-sphere diameter for representing the repulsive force. These modifications are at best semiempirical and do not fix the fundamental problems of MFT [12]. Recently, a modified MFT was proposed by Katsov and Weeks [13,14] by adopting the so-called effective reference field or the effective external potential. This theory was further modified by Huang and Chandler [15]. In order to generate the effective self-consistent field, the modified MFT needs to solve two coupled integral equations simultaneously and reconcile with the bulk fluid behavior by an empirical input of the LJ equation of state. The approach has successfully addressed interfacial and hydrophobic phenomena in inhomogeneous fluids, which is hardly expected for a traditional MFT. In other non-mean-field approaches, Tang *et al.* [16] proposed the inhomogeneous Barker-Henderson (BH) theory, which was an extension from the original version [17] for the uniform LJ fluid. This approach preserves the good performance of the BH theory for bulk fluids and shows some improvements over the MFT. Regrettably, the improvements are limited to some cases and not durable in general. For instance, at the highest density ( $T^* = 1.35$ ,  $\rho^* = 0.82$ ) demonstrated in Ref. [16], the BH theory severely exaggerated the density distribution of LJ molecules around hard walls and the exaggeration persists over distances even far away from the surface. More disturbingly, it is sometimes even inferior to the corresponding MFT if the same BH diameter is adopted, as shown later on. More sophisticated DFT theories have been proposed recently to take into account correlations in inhomogeneous LJ fluids [18–20]. Most of these theories are derived from either

\*Corresponding author.

Email address: yiping.tang@honeywell.com

weighted density approximation (WDA) or perturbation expansions. While these theories show considerable improvements over MFT in reported cases, their applicability to other geometries is often undisclosed. In addition, all of these methods resort to a numerical solution to the Ornstein-Zernike (OZ) equation for either radial distribution function (RDF) or direct correlation function (DCF) to construct the free-energy functional. Such a construction often demands massive computational effort; moreover, it needs extra inputs and parameters to maintain a consistent application to both bulk and inhomogeneous properties [20]. In addition, a potentially fatal problem emerges when the OZ equation loses the solution [20,21].

Very recently, we presented [9] a new DFT based on the solution of the first-order mean-spherical approximation (FMSA) [22,23], originally developed for homogeneous fluids. In comparison with alternative approaches, FMSA possesses a number of advantages. First, it provides analytical expressions for both RDF and DCF for many conventional intermolecular forces including the LJ potential, thus avoiding expensive numerical work. Second, the first-order solution ensures free from any solution breakdown of the OZ equation. Probably, FMSA is to date one of the most accurate theories for thermodynamic properties of simple fluids, especially for phase diagram and chemical potential. In the DFT, the FMSA was extended for inhomogeneous systems through the so-called energy route, in spirit analogous to the BH theory by Tang *et al.* [16]. For LJ fluids near hard walls and inside slit pores [9], the FMSA gives rather good results and its performance is apparently better than MFT. Nevertheless, the FMSA suffers the same problem as the BH theory does: it yields an exaggerated oscillating density profile at high densities. It is further found that for LJ molecules around colloid particles, it fails to give a reasonable density distribution. These drawbacks suggest that a good homogeneous theory does not warrant better results by a simple inhomogeneous extension, and that there are some inadequacies behind the two DFTs. Since both DFTs are formulated through the energy route, we logically suspect that the energy route is accountable for these problems.

In this work, the free-energy functional is reconstructed through Rosenfeld's perturbative method [24] or the DCF route (DCF-FMSA), since the method requires the bulk fluid DCF as the key input. This is in contrast to our previous energy route FMSA, which makes use of RDF to formulate the functional (RDF-FMSA). The DCF-FMSA preserves all advantages of RDF-FMSA for bulk fluids. The DFT is computationally much more attractive due to the analytical availability of DCF. It is applied to several representative geometries and undergoes the self-consistency test.

## II. THEORY

In general, the intrinsic Helmholtz free energy  $F[\rho(\mathbf{r})]$  in DFT can be split into ideal and excess parts

$$F[\rho(\mathbf{r})] = F^{id}[\rho(\mathbf{r})] + F^{ex}[\rho(\mathbf{r})], \quad (1)$$

where the ideal intrinsic Helmholtz energy  $F^{id}[\rho(\mathbf{r})]$  is exactly given

$$F^{id}[\rho(\mathbf{r})] = kT \int d\mathbf{r} \rho(\mathbf{r}) \{ \ln[\rho(\mathbf{r})\Lambda^3] - 1 \}. \quad (2)$$

In Eq. (2),  $k$  is the Boltzmann constant,  $T$  the absolute temperature, and  $\Lambda$  the thermal wavelength. The excess free energy  $F^{ex}[\rho(\mathbf{r})]$  represents the contribution from intermolecular interactions and its functional form is the central topic of DFT. Once the excess free-energy functional is determined, one finds the density profile by solving the Euler-Lagrange equation,

$$\rho(\mathbf{r}) = \rho_b \exp\left(\beta\mu_{ex} - \beta \frac{\delta F^{ex}[\rho(\mathbf{r})]}{\delta \rho(\mathbf{r})} - \beta V_{ext}(\mathbf{r})\right), \quad (3)$$

where  $V_{ext}(\mathbf{r})$  is the external potential and  $\rho_b$  and  $\mu_{ex}$  are the density and excess chemical potential of the corresponding bulk fluid, respectively.

The excess free-energy functional can be further decomposed into the contributions from the short-ranged repulsion and longer-ranged attraction,

$$F^{ex}[\rho(\mathbf{r})] = F_{rep}^{ex}[\rho(\mathbf{r})] + F_{att}^{ex}[\rho(\mathbf{r})]. \quad (4)$$

The split between the repulsion and attraction for the LJ potential

$$u(r) = 4\epsilon \left( \frac{\sigma^{12}}{r^{12}} - \frac{\sigma^6}{r^6} \right) \quad (5)$$

can be made by the BH theory with an effective diameter [17,26]

$$d = \frac{1 + 0.2977T^*}{1 + 0.33163T^* + 1.047710^{-3}T^{*2}} \sigma, \quad T^* = \frac{kT}{\epsilon}. \quad (6)$$

The hard-sphere system with the BH diameter can reasonably represent the repulsive part of the LJ potential, and the representation has been well validated in the homogeneous limit [22,26]. As in the previous work [9], we will apply the MFMT for the functional  $F_{rep}[\rho(\mathbf{r})]$  in Eq. (4). The MFMT functional reduces to the Bounlik-Mansoori-Carnahan-Starling equation of state in the bulk limit, which is consistent with the repulsive part of the homogeneous FMSA. Mathematical expressions of the MFMT functional have been well documented elsewhere and readers may refer to these references for details [7].

To obtain the attractive Helmholtz energy functional, Rosenfeld assumed that it could be perturbatively constructed around that for the bulk fluid at equilibrium [24]. Furthermore, Rosenfeld observed that for charged Yukawa mixtures, the free-energy functional follows the same second-order pattern at both weak (ideal gas) and strong coupling (ideal liquid) limits. Therefore, he deduced that the functional for any attractions can be interpolated by second order and the second-order functional can be constructed by a perturbation expansion around the bulk fluid, i.e.,

$$\beta F_{att}^{ex}[\rho(\mathbf{r})] = \beta F_{att}^{ex}(\rho_b) + \beta \mu_{att}^{ex} \int \Delta\rho(\mathbf{r}_1) d\mathbf{r}_1 - \frac{1}{2} \int c_{att}(\mathbf{r}_1 - \mathbf{r}_2) \Delta\rho(\mathbf{r}_1) \Delta\rho(\mathbf{r}_2) d\mathbf{r}_1 d\mathbf{r}_2, \quad (7)$$

where  $\Delta\rho(\mathbf{r}) = \rho(\mathbf{r}) - \rho_b$ , and the subscript  $b$  stands for the bulk fluid;  $\mu_{att}^{ex}$  and  $c_{att}(\mathbf{r})$  are the attractive part of the excess chemical potential and the DCF of the bulk fluid, respectively. Using a functional expansion [25], Eq. (7) is proven equivalent to the assumption that all the higher-order DCFs are dominated by those of hard spheres. The assumption is further supported by the universality of bridge functions among classical homogeneous fluids observed by Rosenfeld [27]. The observation underlies the reference hypernetted-chain approximation (RHNC) developed some years ago for homogeneous fluids [28].

Equation (7) is appealing for its readiness in numerical implementation: all the inputs are those of the bulk fluid. In particular, the second-order DCF with the relation

$$c(\mathbf{r}_1 - \mathbf{r}_2) = c(|\mathbf{r}_1 - \mathbf{r}_2|) \quad (8)$$

can be obtained from an analytical theory, such as FMSA. The perturbative method is completely free of any weighted

density and of any higher-order DCFs, as appeared in many other DFTs. One also sees that Eq. (7) reduces to the attractive free energy of FMSA at the homogeneous limit, and the basic relation in DFT,

$$\frac{\partial(\beta F_{att}^{ex}[\rho(\mathbf{r})])}{\partial\rho(\mathbf{r}_1)\partial\rho(\mathbf{r}_2)} = -c(\mathbf{r}_1 - \mathbf{r}_2), \quad (9)$$

is held. In implementing Eq. (7), we retrieve the attractive Helmholtz energy and the chemical potential directly from Ref. [22]. The DCF is also derivable as discussed very recently [29]. For the LJ potential, the derivation can be facilitated by its mapping into the two-Yukawa function

$$u(r) = \begin{cases} \infty, & r < d \\ -k_1\epsilon \frac{e^{-z_1(r-d)}}{r} + k_2\epsilon \frac{e^{-z_2(r-d)}}{r}, & r > d \end{cases}, \quad (10)$$

where  $k_1 = k_0 e^{z_1(\sigma-d)}$ ,  $k_2 = k_0 e^{z_2(\sigma-d)}$ ,  $k_0 = 2.1714\sigma$ ,  $z_1 = 2.9637/\sigma$ , and  $z_2 = 14.0167/\sigma$ . This mapping greatly enhances the simplicity of FMSA for thermodynamic properties, RDF, and herein the desired DCF. It can be deduced that the attractive part of the FMSA-DCF is simply given by

$$c_{att}(r) = c_1^{\text{Yukawa}}(T_1^*, z_1 d, r/d) - c_1^{\text{Yukawa}}(T_2^*, z_2 d, r/d), \quad (11)$$

with the definitions of  $T_1^* = T^* d/k_1$  and  $T_2^* = T^* d/k_2$ . The first-order Yukawa DCF can be copied from Ref. [29],

$$rc_1^{\text{Yukawa}}(T^*, z, r) = \begin{cases} \frac{e^{-z(r-1)}}{T^*}, & r > 1 \\ \frac{e^{-z(r-1)}}{T^*} - \frac{1}{(1-\eta)^4 z^6 Q^2(z) T^*} \\ \left\{ S^2(z) e^{-z(r-1)} + 144 \eta^2 L^2(z) e^{z(r-1)} - 12 \eta^2 [(1+2\eta)^2 z^4 + (1-\eta)(1+2\eta) z^5] r^4 \right. \\ \left. + 12 \eta [S(z)L(z) z^2 - (1-\eta)^2 (1+\eta/2) z^6] r^2 - 24 \eta [(1+2\eta)^2 z^4 + (1-\eta)(1+2\eta) z^5] r + 24 \eta S(z)L(z) \right\}, & r \leq 1 \end{cases} \quad (12)$$

with

$$Q(t) = \frac{S(t) + 12 \eta L(t) e^{-t}}{(1-\eta)^2 t^3}, \quad (13)$$

$$S(t) = (1-\eta)^2 t^3 + 6 \eta (1-\eta) t^2 + 18 \eta^2 t - 12 \eta (1+2\eta), \quad (14)$$

$$L(t) = \left(1 + \frac{\eta}{2}\right) t + 1 + 2\eta, \quad \eta = \frac{1}{6} \pi \rho. \quad (15)$$

Note that Eqs. (11) and (12) indicate that

$$c_{att}(r) = -\beta u(r), \quad r > d, \quad (16)$$

which is the first-order approximation to the exact relation

$$c_{att}(r) = \exp[-\beta u(r)] - 1 \quad (17)$$

at the infinite low density. This approximation infers that FMSA and the full MSA, as well, is not accurate at very low densities and temperatures. Nevertheless, the effect on thermodynamic properties is negligible in most circumstances. For instance, phase diagram calculations, which are quite sensitive to low temperatures and densities, can be satisfactorily made by the FMSA [9,22]. It is worth mentioning that the availability of the FMSA-DCF, as is in (12), is guaranteed, while all other methods for obtaining the DCF could face severe challenges in the states near to and below the critical point [29].

### III. RESULTS AND DISCUSSION

In this section, we will demonstrate the applications of the DCF version of FMSA for LJ fluids under a variety of con-

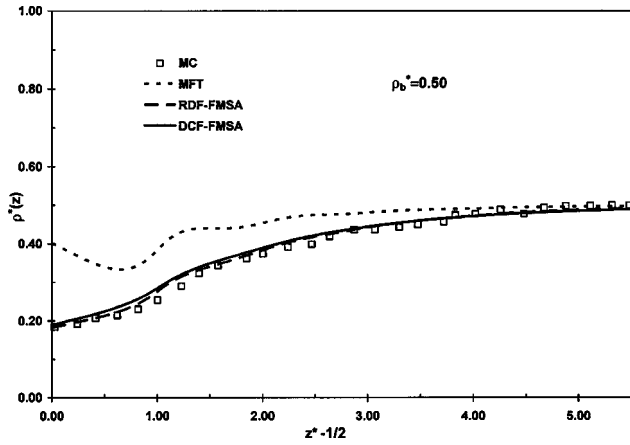


FIG. 1. Density profile ( $\rho^*(z) = \rho(z)\sigma^3$ ,  $\rho_b^* = \rho_b\sigma^3$ ,  $z^* = z/\sigma$ ) of a LJ fluid in contact with a hard wall at  $T^*(kT/\epsilon) = 1.35$ . The symbols are the Monte Carlo (MC) simulation data [31] and three lines are the results of MFT, RDF-FMSA, and DCF-FMSA, respectively.

finements. First, it should be mentioned that all features of the FMSA at the homogeneous limit, as discussed extensively in our earlier RDF version [9], are preserved. These features are crucial to calculating those properties at inhomogeneous conditions such as gas-liquid transition, chemical potential, and so on. Second, in the following DFT applications to inhomogeneous LJ fluids, the corresponding MFT results are also supplied to serve as a comparison. One should be aware that, in order to obtain a meaningful density profile, the chemical potential in the Euler-Lagrange equation has to be calculated accordingly by the MFT at the corresponding bulk density, despite that such a potential is very poor [9]. In addition, our MFT differs from others in the literature not only in the MFMT for the short-ranged repulsion, but also in using the BH diameter and the corresponding split for attraction. By fixing all these conditions identical to each other, we can eliminate any ambiguities in comparing the two theories. Finally, the DCF outside the hard core in Eq. (11) should be replaced by the original LJ potential (5) if its values at  $r > 3\sigma$  are non-negligible [22], and for those systems with a cutoff in computer simulation, one can make a mean-field correction to compensate the cutoff effect as done by others [20].

### A. Near hard walls

These systems were studied in our RDF version of FMSA for the reduced bulk density  $\rho^* (= \rho\sigma^3)$  0.5 and 0.65, as well as by Tang *et al.* [16], using the BH perturbation theory. In addition to MFT, the results of RDF-FMSA are also plotted for comparison. Figures 1 and 2 suggest that both DCF-FMSA and RDF-FMSA successfully account for the depletion around the solid-fluid interface and that their performance is quantitatively satisfactory. In contrast, the MFT is not only quantitatively unreliable but also qualitatively questionable, because it fails to represent the depletion, and the density oscillation cannot be sufficiently suppressed. Clearly, the MFT problems are caused by its structureless free-energy functional, while the structure is well represented in

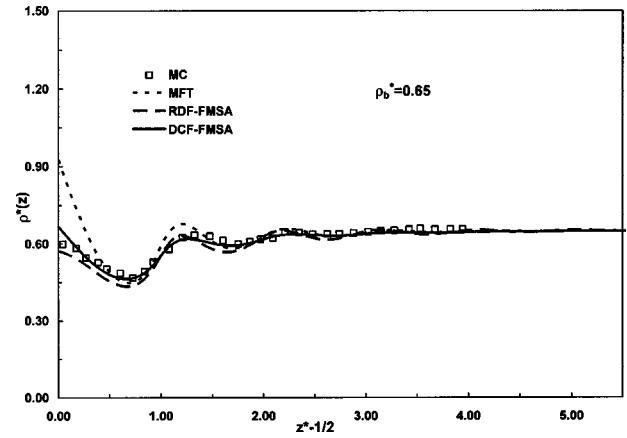


FIG. 2. The same as in Fig. 1 except at a moderate bulk density.

FMSA—either through RDF or DCF. The poor performance of MFT was repeated for Yukawa molecules in contact with the hard wall [25], where the depletion emerges at low temperatures. Comparing the two versions of FMSA at the two densities, the DCF version appears slightly better, as shown in Fig. 2.

However, the good impression about RDF-FMSA is not sustainable at high densities. The finding in Fig. 3 at  $\rho^* = 0.82$  is very striking: the RDF-FMSA severely exaggerates the density oscillation and the exaggeration persists over large distances, while the computer simulation reveals that the oscillation is rapidly suppressed. This magnitude and persistence of oscillation were also shared by the BH theory [16]. Somehow unexpectedly, the MFT yields a quite good density profile, especially in suppressing the oscillation, despite its poor performance at the two other densities. It should be pointed out that this observation is contrary to that of Tang *et al.* [16] regarding MFT. The present MFT is implemented by making use of the BH parameter and the MFMT for the repulsive functional, while Tang *et al.* [16] utilized the unit diameter and a WDA for the repulsive part. Obviously, using the same BH diameter is much fairer in comparison. The findings in Fig. 3 infer that the RDF or energy route to construct the free-energy functional is sound at low and moderate densities but could go astray at high

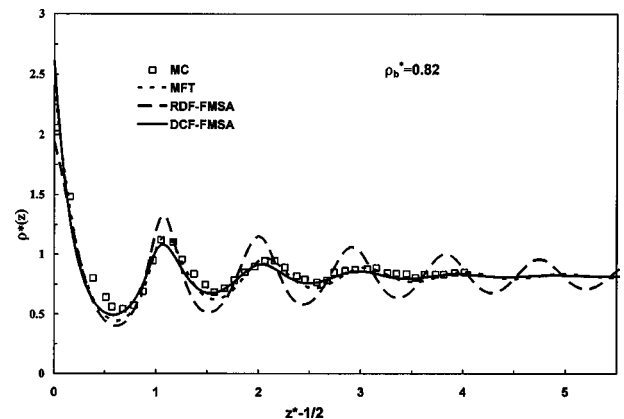


FIG. 3. The same as in Fig. 1 except at a high bulk density.

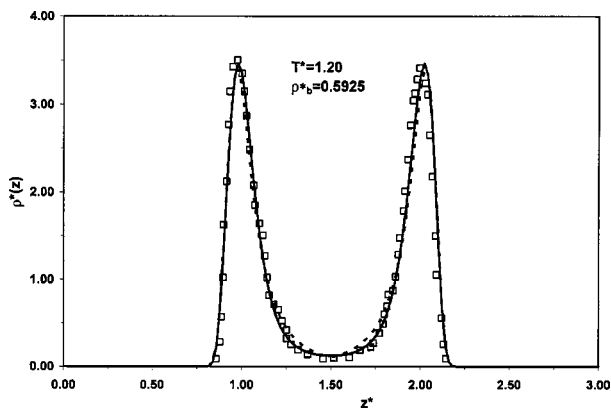


FIG. 4. Density profile of a LJ fluid inside a slit pore  $H^* = H/\sigma = 3.0$ . The symbols are the computer simulation data [30]. The solid and dashed lines are the predictions of the FMSA and MFT, respectively.

densities, where the attraction role should be diminished. Conversely, MFT poorly takes into account the attractive force but the account happens to be right at high densities. In contrast to the two unstable theories, the DCF-FMSA is as good as in Figs. 1 and 2 and suppresses successfully the oscillation. In a separate investigation [25], the DCF-FMSA is found equally stable for inhomogeneous Yukawa fluids from low to high temperatures. Therefore, throughout the remaining part of this paper, we will test only the DCF version of FMSA and refer to it as FMSA for brevity.

### B. Inside slit pores

Figures 4–7 give the density profiles of LJ fluids in attractive slit pores with the width  $H^*$  ( $=H/\sigma$ ) = 3, 4, 5, and 7.5, respectively. The interaction between LJ molecules and the wall is simulated by Steele's 10-4-3 potential,

$$V_s(z) = \varepsilon_w \left[ \frac{2}{5} \left( \frac{\sigma_w}{z} \right)^{10} - \left( \frac{\sigma_w}{z} \right)^4 - \frac{\sigma_w^4}{3\Delta(z+0.61\Delta)^3} \right], \quad (18)$$

in which the parameters are related to those of the LJ potential by

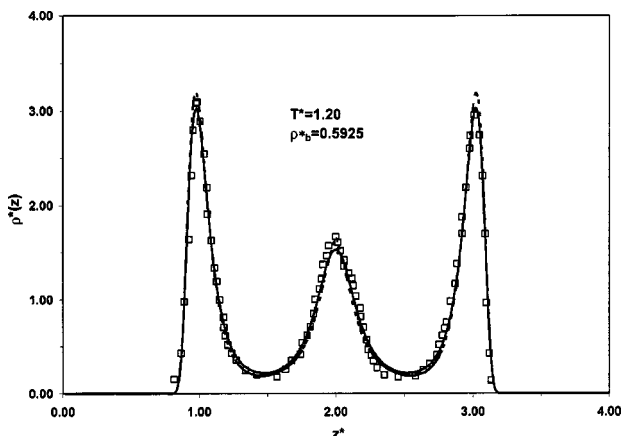


FIG. 5. The same as in Fig. 4 except  $H^* = 4$ .

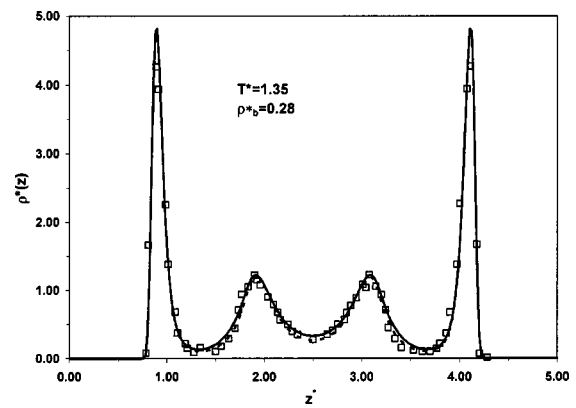


FIG. 6. The same as in Fig. 4 except  $H^* = 5$  and the simulation data [32].

$$\sigma_w = \sigma, \quad \varepsilon_w = 6.283\varepsilon, \quad \Delta = 0.7071\sigma \quad (19)$$

for  $H^* = 3, 4, 7.5$ , and

$$\sigma_w = 0.903\sigma, \quad \varepsilon_w = 12.96\varepsilon, \quad \Delta = 0.8044\sigma \quad (20)$$

for  $H^* = 5$ . In these slits, the external potential in the Euler-Lagrange equation should read

$$V_{ext}(z) = V_s(z) + V_s(H - z). \quad (21)$$

Besides computer simulations [30,32,33], a number of models have been developed for these attractive slit pores. Vanderlick *et al.* [34] compiled the results of several typical earlier models: the generalized van der Waals, generalized hard-rod, and Tarazona and Yvon-Born-Green for  $H^* = 3, 4$ . Kierlik and Rosinberg [35] studied these systems by a scalar version of FMT and a modified hard-sphere diameter, which fits better liquid densities of phase coexistence. Using the same modified diameter, Choudhury and Ghosh [19] studied these pores by constructing the hard-sphere free-energy functional through a third-order DCF. Note that all of these studies were concentrated only on the repulsive functional and treated the attractive part in a mean-field manner.

Figures 4–7 suggest that the performance of the FMSA is overall comparable to that of the MFT, of which the FMSA yields a better density profile for  $H^* = 3$  and slightly under-

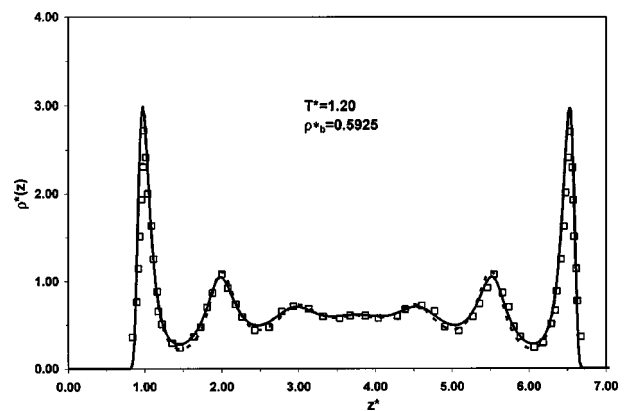


FIG. 7. The same as in Fig. 4 except  $H^* = 7.5$  and the simulation data [33].

estimates the density peaks for  $H^*=4$ . If compared with those DFT models studied by Vanderlick *et al.* [34], in which their quantitative performance is far from satisfactory our FMSA is much better. It appears that the MFT of Kierlik and Rosinberg [35] resembles much the present MFT, since both of them are based on FMT. The theory of Choudhury and Ghosh [19] is also satisfactory, but conspicuously underestimates these peaks in  $H^*=5.0$ . In general, the FMSA is as good as the theory of Kierlik and Rosinberg, and of Choudhury and Ghosh. It is proper to remind that these apparently similar performances should not undermine the fundamental difference between the FMSA and those mean-field approaches: the FMSA with the rigorously derived BH diameter is very reliable at the bulk limit, while the applicability of those MFTs with a forged diameter is questionable.

### C. Around colloid particles

The colloid particle discussed here is simply represented by a hard-sphere solute with varying size, surrounded by the LJ molecules. The introduced external potential reads

$$V_{ext}(r) = \begin{cases} \infty, & r/\sigma < S \\ 0, & r/\sigma > S \end{cases}, \quad (22)$$

in which  $S$  is the dimensionless distance between the particle and a LJ molecule. The inhomogeneous system exhibits an interesting phenomenon that resembles the hydrophobic effects. Close to the particle with a size comparable to a LJ molecule, the density profile is highly oscillatory and very much like a RDF of the LJ fluid. With the increasing particle size, however, the oscillation rapidly fades away and a drying layer with a vapor-like density is formed around the particle surface. If the particle is large enough, the recovery from the drying layer to the bulk density over space can be essentially monotonous. To a large extent, this behavior is similar to that of LJ molecules around hard walls discussed earlier. In fact, a wall can be viewed as a special sphere of infinite diameter.

Figure 8 shows that our FMSA is able to account for the aforementioned phenomenon: The drying process with the increasing particle size is successfully reproduced and the agreement between the theory and computer simulation [36] is excellent. In contrast, the density profiles from the MFT are highly oscillatory in all cases and their first peaks always occur at the contact. Again, this behavior is quite similar to what we saw earlier for hard walls. Therefore, it is conclusive that a plain MFT is incapable of showing depletion around hard walls or hard spheres. Since the only difference between the FMSA and the MFT is the DCF, one can deduce that a reliable DCF is essential to account for depletion within the framework of the present DFT. It is noted that the modified MFT [13] can also successfully address the size-induced drying phenomena due to the adoption of the effective external potential.

### D. Self-consistency test

The self-consistency test can be easily performed by fixing an LJ molecule at the origin, or by setting the external

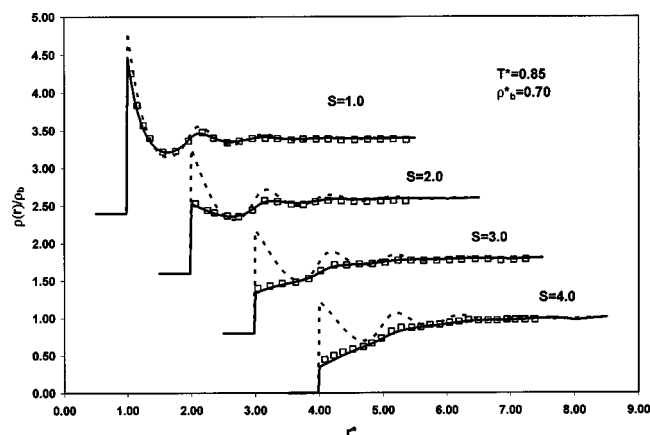


FIG. 8. Density profiles ( $r^* = r/\sigma$ ) of a LJ fluid around colloid particles with different sizes. The symbols are the computer simulation data [36]. The solid and dashed lines are the predictions of the FMSA and MFT, respectively. To enhance visual clarity, the profiles of  $S=1, 2,$  and  $3$  are shifted upward by  $2.4, 1.6,$  and  $0.8,$  respectively.

potential in Eq. (22) the same as the LJ potential. The resulting density profile should provide the structural information of the bulk LJ fluid through the relation  $g(r) = \rho(r)/\rho_b$ . However, since the density profile is solved from the Euler-Lagrange equation, while the conventional RDF is obtained by solving the OZ equation or by the homogeneous FMSA, the two pieces of information do not necessarily coincide with each other. Therefore, the degree of coincidence between the two functions will reveal the global consistency of our FMSA. The results of the two functions, together with computer simulation data [37], are depicted in Fig. 9. There is an excellent agreement between the RDF of density profile and that of the homogeneous FMSA, with only minor discrepancies near the first peak. In addition, these results are in very good agreement with computer simulation data, demonstrating the high fidelity of FMSA. It is notable that the temperature and density in the Fig. 9 is very close to the triple point of the LJ fluid, and the observed consistency and accuracy are more persuasive than other states.

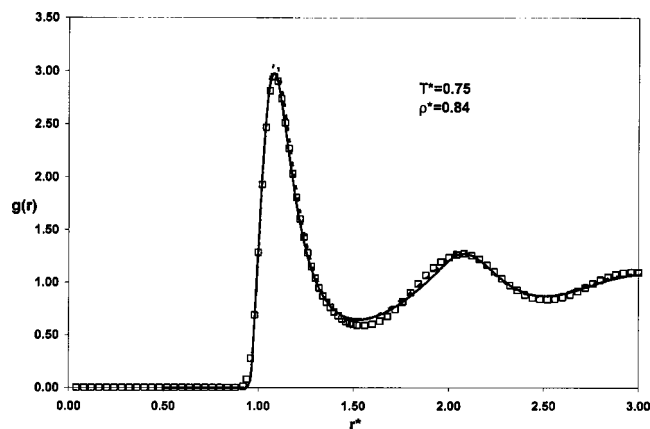


FIG. 9. Consistency test between RDF from the FMSA density profile (solid line) and from the homogeneous FMSA (dashed line). The symbols are the computer simulation data [37].

Rosenfeld also conducted [38] a similar consistency test based on the hard-sphere free-energy functional from the original FMT and the DCF from the RHNC approximation. While the resulting RDF is apparently very close to what we achieve here, Rosenfeld's method is computationally much more cumbersome: the hard-sphere diameter has to be determined implicitly inside an integral, and a numerical solution to the RHNC has to be performed. Note that these burdens are fully waived within the FMSA.

#### IV. CONCLUSION

Rosenfeld first proposed [24] the perturbative method to treat the attractive functional by making use of the DCF of the corresponding bulk fluid. He argued that this treatment is simpler than all other DFTs in the literature and is theoretically justified due to its plain interpolation between the ideal-gas and "ideal-liquid" limits. Since then, however, this method has found no further elaboration except one application to homogeneous fluids [38]. This absence is caused, at least in part, by insufficient and inaccurate knowledge about the attractive DCF. Rosenfeld's prescription for the DCF is to solve simultaneously the OZ and the Euler-Lagrange equations. The prescription is computationally quite expensive and may face deadlock if the solution to the OZ equation is unattainable. It remains unclear to what extent Rosenfeld's prescription can be applied to inhomogeneous fluids.

In this work, we made two modifications in implementing Rosenfeld's method: the hard-sphere functional is replaced

by the more accurate MFMT and the attractive functional by the FMSA-DCF. These modifications tremendously reduce the computation work and avoid potential numerical breakdown. In particular, since the FMSA-DCF is analytically attainable, the implementation of the FMSA is as comfortable and efficient as of the MFT.

Our FMSA has been applied to several representing inhomogeneous systems, including LJ molecules near hard walls, inside silt pores, and around colloid particles. The theory successfully remedies the deficiencies of its earlier RDF version and is capable of describing the surface depletion of LJ fluids. In contrast, the widely used MFT, although good for confined attractive surfaces such as slits, fails to account for the depletion. The FMSA is also highly self-consistent in the sense that it yields almost an identical RDF from two different routes. The quantitative performance of the FMSA, is at least comparable to several other theories reported individually for these systems. Therefore, the FMSA developed in this work is comprehensively reliable and computationally efficient. Together with its exclusive advantages at the homogeneous limit, the FMSA is very promising for practical applications.

#### ACKNOWLEDGMENTS

J.W. gratefully acknowledges the financial support of the University of California Research and Development Program and the National Science Foundation (Grant No. CTS-0340948).

- 
- [1] R. Evans, *Fundamentals of Inhomogeneous Fluids*, edited by D. Henderson (Dekker, New York, 1992).
- [2] Y. Rosenfeld, *Phys. Rev. Lett.* **63**, 980 (1989).
- [3] Y. Rosenfeld, *J. Chem. Phys.* **92**, 6819 (1990); **93**, 4305 (1990).
- [4] Y. Rosenfeld, *Phys. Rev. A* **42**, 5978 (1990).
- [5] Y.-X. Yu and J. Wu, *J. Chem. Phys.* **116**, 7094 (2002).
- [6] Y.-X. Yu and J. Wu, *J. Chem. Phys.* **117**, 2368 (2002).
- [7] Y.-X. Yu and J. Wu, *J. Chem. Phys.* **117**, 10156 (2002).
- [8] R. Roth, R. Evans, A. Lang, and G. Kahl, *J. Phys.: Condens. Matter* **14**, 12063 (2002).
- [9] Y. Tang and J. Wu, *J. Chem. Phys.* **119**, 7388 (2003).
- [10] B. Q. Lu, R. Evans, and M. M. Telo da Gama, *Mol. Phys.* **55**, 1319 (1985).
- [11] E. Velasco and P. Tarazona, *J. Chem. Phys.* **91**, 7916 (1989).
- [12] P. I. Ravikovitch, A. Vishnyakov, and A. V. Neimark, *Phys. Rev. E* **64**, 011602 (2001).
- [13] K. Katsov and J. D. Weeks, *J. Phys. Chem. B* **105**, 6738 (2001).
- [14] K. Katsov and J. D. Weeks, *J. Phys. Chem. B* **106**, 8429 (2002).
- [15] D. M. Huang and D. Chandler, *J. Phys. Chem. B* **106**, 2047–2053 (2002).
- [16] Z. Tang, L. E. Scriven, and H. T. Davis, *J. Chem. Phys.* **95**, 2659 (1991).
- [17] J. A. Barker and D. Henderson, *J. Chem. Phys.* **47**, 2856 (1967); **47**, 4714 (1967).
- [18] S. Zhou and E. Ruckenstein, *J. Chem. Phys.* **112**, 5242 (2000).
- [19] N. Choudhury and S. K. Ghosh, *Phys. Rev. E* **64**, 021206 (2001).
- [20] M. B. Sweatman, *Phys. Rev. E* **63**, 031102 (2001).
- [21] G. Sarkisov, *J. Chem. Phys.* **114**, 9496 (2001).
- [22] Y. Tang, Z. Tong, and B. C.-Y. Lu, *Fluid Phase Equilib.* **134**, 21 (1997); **190**, 149 (2001).
- [23] Y. Tang and B. C.-Y. Lu, *AIChE J.* **43**, 2215 (1997).
- [24] Y. Rosenfeld, *J. Chem. Phys.* **98**, 8126 (1993).
- [25] Y. Tang, *J. Chem. Phys.* (unpublished).
- [26] Y. Tang, *J. Chem. Phys.* **116**, 6694 (2002).
- [27] Y. Rosenfeld and N. W. Ashcroft, *Phys. Rev. A* **20**, 1208 (1979).
- [28] F. Lado, *Phys. Lett.* **89A**, 196 (1982).
- [29] Y. Tang, *J. Chem. Phys.* **118**, 4140 (2003).
- [30] J. J. Magda, M. Tirrell, and H. T. Davis, *J. Chem. Phys.* **83**, 1888 (1985).
- [31] C. Balabanic, B. Borstnik, R. Milcic, A. Rubcic, and F. Sokolic, in *Static and Dynamic Properties of Liquids*, edited by M. Davidoviv and A. K. Soper, Springer Proceedings in Physics (Springer, Berlin, 1989), Vol. 40 and p. 70.
- [32] J. P. R. B. Walton and N. Quirke, *Chem. Phys. Lett.* **129**, 382 (1986).
- [33] I. K. Snook and W. Van. Meegen, *J. Chem. Phys.* **72**, 2907

- (1980); **74**, 1409 (1981).
- [34] T. K. Vanderlick, L. E. Scriven, and H. T. Davis, *J. Chem. Phys.* **90**, 2422 (1989).
- [35] E. Kierlik and M. L. Rosinberg, *Phys. Rev. A* **44**, 5025 (1991).
- [36] D. M. Huang and D. Chandler, *Phys. Rev. E* **61**, 1501 (2000).
- [37] L. Reatto, D. Levesque, and J. J. Weis, *Phys. Rev. A* **33**, 3451 (1986).
- [38] Y. Rosenfeld, *Mol. Phys.* **94**, 929 (1998).